Electronic Supplementary Material (ESI) for RSC Advances.
This journal is © The Royal Society of Chemistry 2015

Supplementary Information:

Nanostructured cobalt phosphide-based films as bifunctional electrocatalysts for overall water splitting

Julian A. Vigil and Timothy N. Lambert*

Department of Materials, Devices & Energy Technologies, Sandia National Laboratories, Albuquerque, New Mexico, 87185, USA
*Fax: 505 844 7786; Tel: 505 284 6967; E-mail: tnlambe@sandia.gov.

* Author to whom correspondences should be addressed

Abbreviations:
SEM = Scanning electron microscopy
GIXRD = Grazing incidence x-ray diffraction
XPS = X-ray photoelectron spectroscopy
HER = Hydrogen evolution reaction
OER = Oxygen evolution reaction
ECSA = Electrochemically active surface area
RF = Roughness factor
RDV = Rotating disk voltammetry
CV = Cyclic voltammetry
C_{DL} = Double layer capacitance
C_S = Specific capacitance
A = geometric area
η = Overpotential
b = Tafel slope
NR = Not reported
NA = Not attained

Experimental

General

All chemicals were obtained commercially and used as received, without further purification. Cobalt(II) nitrate hexahydrate ($Co(NO_3)_2 \bullet 6H_2O$) was purchased from Alfa Aesar. Sodium nitrate ($NaNO_3$) was purchased from Fisher Scientific. Sodium hypophosphite monohydrate ($NaH_2PO_2 \bullet H_2O$) was purchased from Alfa Aesar. Ethyl alcohol (200 proof) was purchased from Pharmco-Aaper. Nickel foil (0.05 mm thick, 99+% metals basis) and titanium foil (0.032 mm thick, 99.7% metal basis) were purchased from Alfa Aesar. Co_3O_4 from Alfa Aesar was also used in control experiments. Gold-coated nickel foil (Au/Ti/Ni) was prepared as follows: Ni foil was cleaned with acetone, methanol, and isopropyl alcohol and dried under a stream of N_2. The Ni foil was then fixed to a 6" platen, placed in a Temescal eBeam FC-2000 evaporator, pumped to ultra-high vacuum (5 x 10^{-7} Torr), and a Ti/Au stack was deposited at 50 Å Ti, then 500 Å Au.

Materials Characterization

Grazing-Incidence X-ray Diffraction (GIXRD): A Siemens model D500 θ-2θ powder diffractometer (Bruker AXS, Inc. Madison, WI) was used for GIXRD data collection with samples maintained at room temperature (25°C). Copper Kα (0.15418 nm) radiation was produced via a sealed-tube X-ray source and a diffracted-beam curved graphite monochromator; a conventional scintillation counter was used as the detector. Fixed 0.3° incident beam and scatter slits were used (goniometer radius = 120 mm), and the instrument power settings were 40 kV and 30 mA. Powder diffraction patterns were collected using a grazing angle of 2.0° θ. The patterns were collected using the following parameters: 10-80° 2θ range, step-size of 0.05° 2θ and a count time of 30 seconds.

Scanning Electron Microscopy (SEM): The samples were imaged using a Zeiss Supra 55VP field emitter gun scanning electron microscope (FEGSEM).

X-ray Photoelectron Spectroscopy (XPS): Samples were analyzed via XPS at pressures less than 5 x 10^{-9} Torr. XPS was performed using a Kratos Axis Ultra DLD instrument using monochromatic Al Kα (1486.7 eV) source. The analysis area was an elliptical spot size of 300 x 700 microns. Several locations on each sample were analyzed to obtain a representative sampling. Survey spectra were recorded with an 80

eV pass energy, 500 meV step sizes, and 100 ms dwell times. High resolution spectra were recorded with a 20 eV pass energy, 50 meV step sizes, and 100 ms dwell times. Charge neutralization was used for all samples to reduce any potential differential charging effects. Data processing was performed with CasaXPS Version 2.3.15. High resolution core-level peaks were compared by normalizing counts for each respective core-level.

CoP Synthesis

Co_3O_4 films with a known mass loading of 25 μg were prepared using a two-step electrodeposition-thermal annealing method as recently described.[1] The substrate was Ni foil, Ti foil, or Au-coated Ni foil. A Co_3O_4/substrate sample (or substrate only as a control) was then placed on a small pedestal (film side up) within the crucible and surrounded with 0.5 g NaH_2PO_2 as shown in Fig. S1. The crucible was covered and then transferred to a small box furnace inside a glove box filled with an inert atmosphere of Ar gas. The furnace was rapidly heated to 300 °C (at ~ 34 °C min^{-1}) and then held at that temperature for 2 h after which time the sample was allowed to cool to ambient temperature and then removed for analysis. CoP loadings are calculated to be 28 μg or 143 μg cm^{-2}.

Control Film and Powder Synthesis

Blank Ni, Ti, and Au foil substrates were reacted in an identical manner to the Co_3O_4 films. Commercial Co_3O_4 was mixed with the NaH_2PO_2, heated to 300 °C (as described above), washed with water and then dried. Ni, Ti, and Au foils after undergoing the phosphidation reaction are denoted as Ni*, Ti*, and Au* in the following figures.

Electrochemical Studies

Hydrogen and oxygen evolution rotating disc electrode (RDE) experiments were performed in a three-electrode cell connected to a Radiometer Analytical PGZ100 All-In-One Potentiostat. The rotation rate of the working electrode (EDI101, Radiometer Analytical), was controlled by a speed control unit (CTV101, Radiometer Analytical). For electrochemical analyses, the samples were housed in an adaptor [Radiometer Analytical, EM-EDI-SMP Disc Sample Holder Tip for EDI Rotating Disc Electrode (d=11 mm)] that was connected to the EDI101. The exposed geometric area of the film was 0.1963 cm^2. The counter electrode was Pt in alkaline electrolyte and a graphite rod in

acidic electrolyte. The reference electrode was Hg/HgO (0.1 M KOH, Hach) or $Hg/HgSO_4$ (saturated K_2SO_4, Hach). The electrolytes used were 0.5 M H_2SO_4 (HER), 0.1 M KOH (HER and OER), and 1 M KOH (HER, OER, and electrolysis) that had been thoroughly purged with N_2 for $\geq$ 20 minutes prior to the initiation of the experiment. The gaseous atmosphere was maintained for the duration of the experiment via blanketing. Electrochemical HER and OER were evaluated by rotating disc voltammetry (RDV) in the specified electrolyte, with a scan rate of 5 mV s^{-1} and rotation rate of 1600 RPM. Only a portion of the forward scan of each RDV experiment is shown in plots, for the sake of presentation. HER RDV scans were run from ~0.2 V vs. RHE to the voltage at which they achieved ~20 mA cm^{-2} to avoid the accumulation of H_2 gas on the catalyst surface. OER RDV scans were run from 0.94 V to 2.14 V vs. RHE. Stability experiments were performed with 100-cycle RDV experiments (in the same window as the initial RDV scan) at a scan rate of 50 mV s^{-1} for HER, and a 2 hour galvanostatic hold at 10 mA cm^{-2} for OER. Data was analyzed using Voltamaster 4 software and plotted for presentation purposes using Kaleidagraph software.

Water electrolysis was investigated in similar fashion to a previous report.[2-3] Experiments were performed in a two-electrode cell connected to a Princeton Applied Research Potentiostat/Galvanostat Model 273. A CoP/Au or CoP/Ni film operated as both the working and counter electrode to demonstrate the OER-HER bi-functionality of these catalysts. 1 M KOH was used as the electrolyte. A RDV scan was run from 0 V, past the theoretical thermodynamic equilibrium cell voltage of 1.23 V, to 2 V in order to record the potential at which the current density reached 10 mA cm^{-2}. A galvanostatic experiment was then run at 10 mA cm^{-2} to assess the device's stability. Care was taken to minimize gas accumulation at the anode or cathode which can interfere with the experiment due to transport-related resistances. Data was analyzed using CorrView software and plotted for presentation purposes using Kaleidagraph software.

Onset potentials were calculated by the tangential method as previously reported.[1] The intersection of the two slopes, one in the pre-onset non-faradaic region and the other in the post-onset reaction region of the curve, was defined as the onset potential. This method likely underestimates the onset potential relative to the classic, widely used definition, but it was found to be a more consistent for comparison purposes.

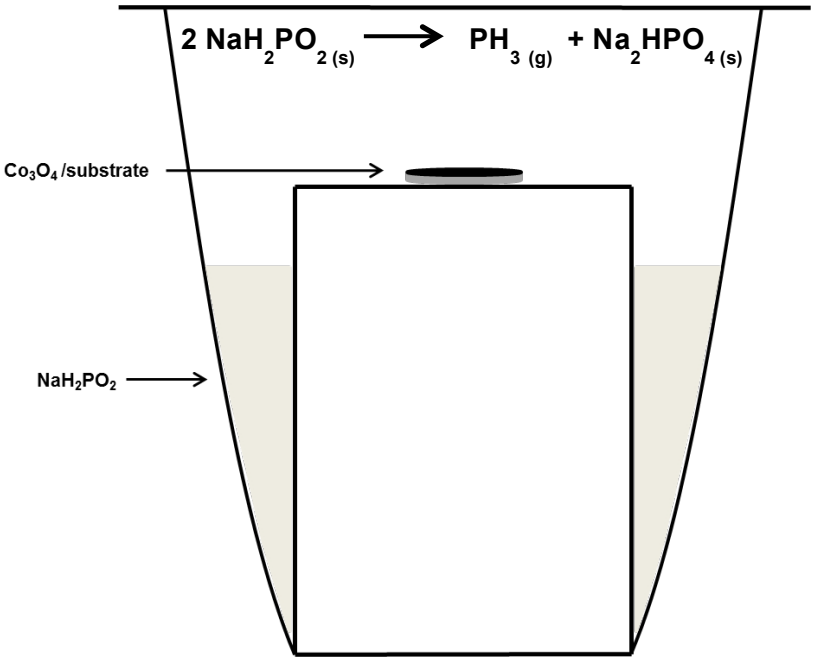

Fig. S1 Schematic of crucible/pedestal arrangement in the phosphidation reaction. Set-up allows close proximity of NaH_2PO_2 and Co_3O_4/substrate precursors while eliminating direct contact and providing a minimal reaction volume space.

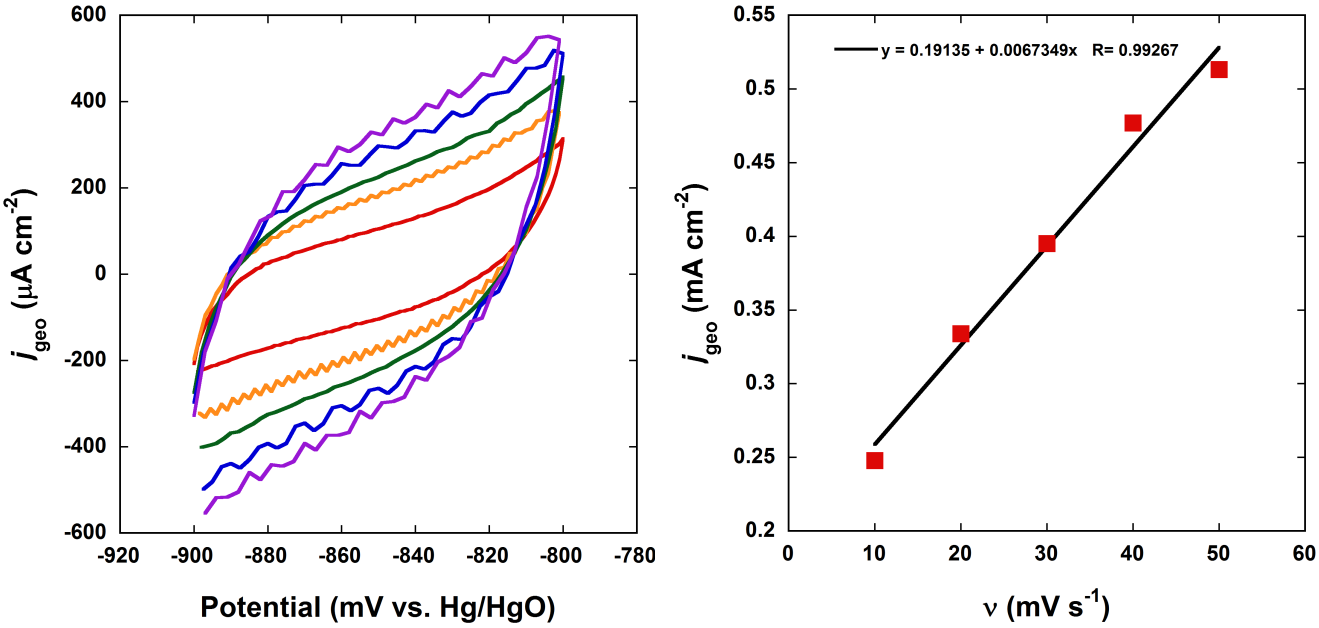

Fig. S2 Electrochemically active surface area (ECSA) determination for CoP/Ni. CV scans (left) were run in a non-faradaic region corresponding to double-layer charging, or capacitance, prior to the onset of hydrogen evolution. Scan rate (ν) was increased in 10 mV s^{-1} increments from 10 to 50 (red to purple) mV s^{-1} for each scan to monitor the change in current density in the region. A value of -810 mV vs. Hg/HgO was chosen as a value, within 20% of the anodic switching potential, to examine the dependency of current density on scan rate (right). The slope of the ν vs. j_{geo} (geometric current) gives the capacitance, from which ECSA and roughness factor (RF) can be calculated (below). C_{DL} = Double layer capacitance, C_S = specific capacitance, A = geometric area.

$$\text{Slope} = 0.0067349 \text{ (mA s mV}^{-1}\text{ cm}^{-2}\text{)} = 0.0067349 \text{ F cm}^{-2}$$

$$C_{DL} = 0.0067349 \text{ F cm}^{-2} \bullet 0.1963 \text{ cm}^2 = 0.001322 \text{ F}$$

$$\text{ECSA} = C_{DL}/C_S = 0.001322 \text{ F}/0.00004 \text{ F cm}^{-2} = 33.1 \text{ cm}^2$$

$$\text{RF} = \text{ECSA}/A = 33.1 \text{ cm}^2/0.1963 \text{ cm}^2 = 168.4$$

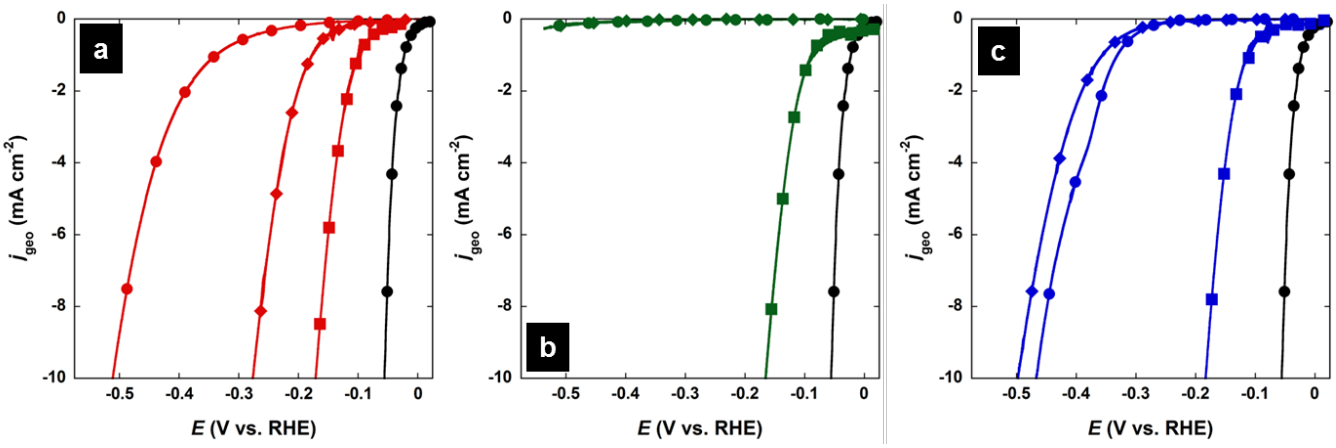

Fig. S3 Comparison of CoP/substrates and 20% Pt/C with control samples for HER in 0.5 M H_2SO_4. (a) RDV scan of blank Ni foil (red, filled circles), Ni* (red, filled diamonds), CoP/Ni (red, filled squares) and 20% Pt/C. Increased activity of Ni* foil is proposed to be the surface formation of Ni_2P, which is known to be active for the HER;[4-5] (b) RDV scan of blank Ti foil (green, filled circles), Ti* (green, filled diamonds), CoP/Ti (green, filled squares) and 20% Pt/C; (c) RDV scan of blank Au foil (blue, filled circles), Au* (blue, filled diamonds), CoP/Au (blue, filled squares) and 20% Pt/C.

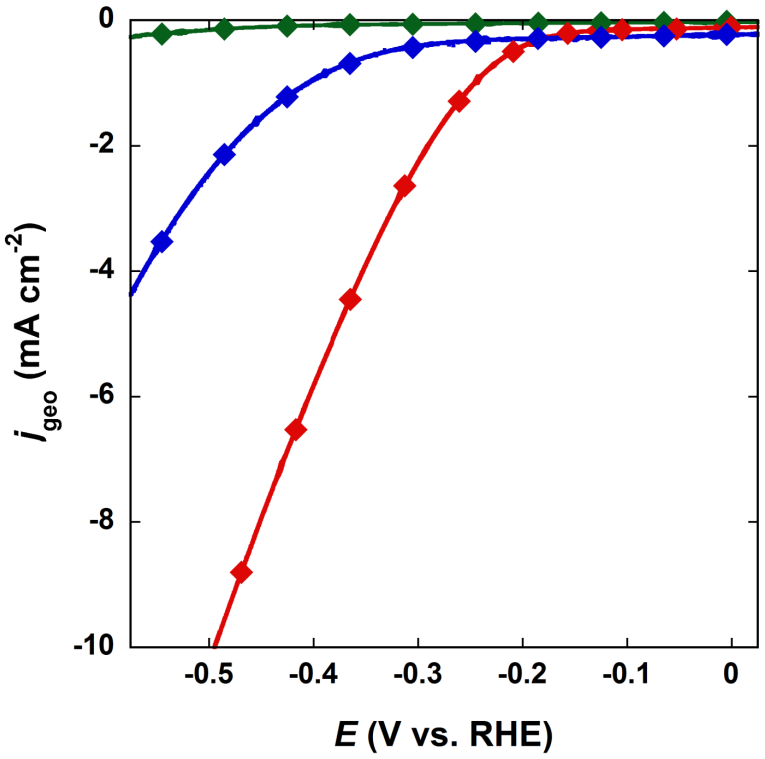

Fig. S4 Control samples for HER in 0.1 M KOH. RDV scans of Ti* (green, filled diamonds) Au* (blue, filled diamonds) and Ni* (red, filled diamonds).

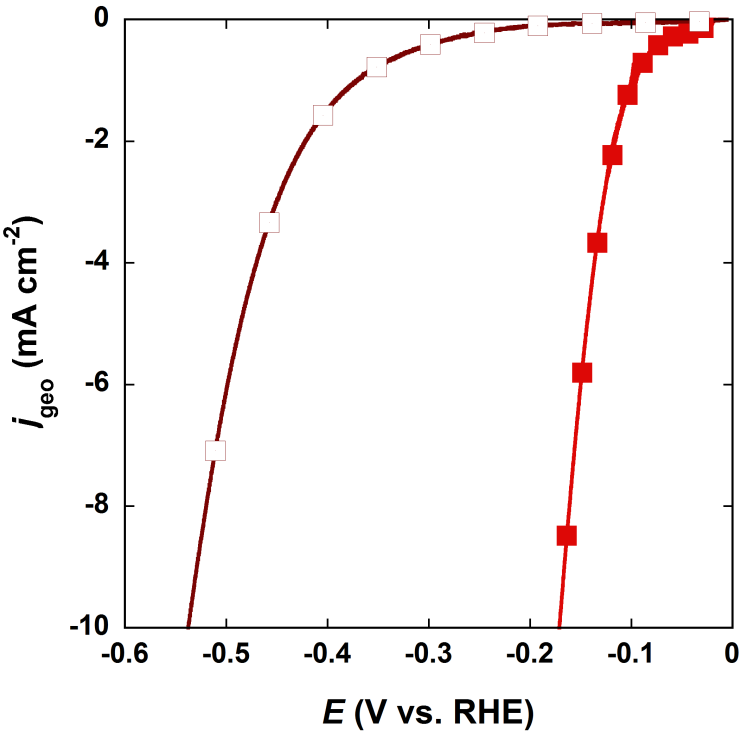

Fig. S5 Precursor Co_3O_4 film for HER in 0.5 M H_2SO_4. RDV scans of Co_3O_4/Ni (brown, open squares) and Co-PP/Ni (red, closed squares).

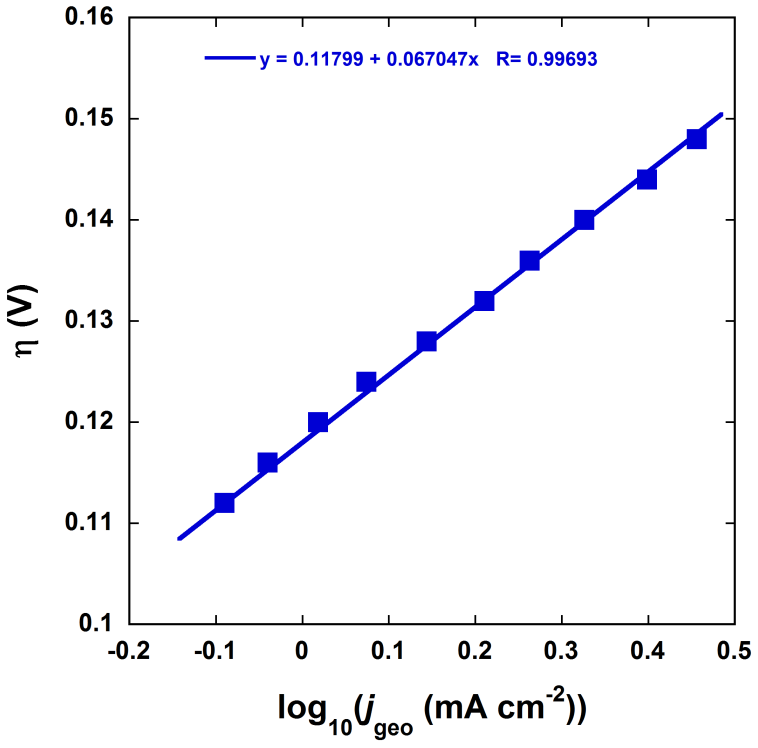

Fig. S6 Tafel plot and slope (67 mV decade^{-1}) for Co-PP/Au in 1 M KOH.

Table S1 Comparison of comparable state of the art HER-OER bifunctional catalysts.

	Substrate/ catalyst loading (mg cm^{-2})	$\eta_{10\ mA}$ (V) HER 0.5 M H_2SO_4	b (mV dec^{-1}) HER 0.5 M H_2SO_4	$\eta_{10\ mA}$ (V) HER 1 M KOH	b (mV dec^{-1}) HER 1 M KOH	$\eta_{10\ mA}$ (V) OER 1 M KOH	$\eta_{10\ mA}$ (V) symmetrical electrolysis 1 M KOH
Co-PP/Au[this work]	Au/ 0.14	0.183	59	0.196	67	0.34	0.41-0.51
PCPTF[6]	Au/ 0.1	0.150‡	53	0.375‡	NR	0.30‡	NR
Co_3O_4 NCs[3]	CF/ 0.35	NR	NR	NA	116	0.32‡	0.68
CoOx@CN[2]	C/ 0.42	NR	NR	0.232	115	0.40‡	0.4-0.5Ψ
Co-P[7]	Cu/ 1.0	NR	NR	0.094	42	0.35	0.42‡
Co@N-C[8]	C/ NR	NR	NR	0.21	108	0.42	NR

η = Overpotential; b = Tafel slope; NR = not reported; NA = not attained; CF = carbon fiber; C = N-doped carbon. ‡Values have been approximated from figures in the cited texts. ΨOverpotential value provided in this text was at 20 mA cm^{-2} presumably due to highly offset RDV scan.

Notes and References

1 T. N. Lambert, J. A. Vigil, S. E. White, D. J. Davis, S. J. Limmer, P. D. Burton, E. N. Coker, T. E. Beechem and M. T. Brumbach, *Chem. Commun.*, 2015, **51**, 9511-9514.

2 H. Jin, J. Wang, D. Su, Z. Wei, Z. Pang and Y. Wang, *J. Am. Chem. Soc.*, 2015, **137**, 2688-2694.

3 S. Du, Z. Ren, J. Zhang, J. Wu, W. Xi, J. Zhu and H. Fu, *Chem. Commun.*, 2015, **51**, 8066-8069.

4 A. Lu, Y. Chen, H. Li, A. Dowd, M. B. Cortie, Q. Xie, H. Guo, Q. Qi and D.-L. Peng, *Int. J. Hydrogen Energ.*, 2014, **39**, 18919-18928.

5 E. J. Popczun, J. R. McKone, C. G. Read, A. J. Biacchi, A. M. Wiltrout, N. S. Lewis and R. E. Schaak, *J. Am. Chem. Soc.*, 2013, **135**, 9267-9270.

6 Y. Yang, H. Fei, G. Ruan and J. M. Tour, *Adv. Mater.*, 2015, **27**, 3175-3180.

7 N. Jiang, B. You, M. Sheng and Y. Sun, *Angew. Chem. Int. Ed.*, 2015, **54**, 6251-6254.

8 J. Wang, D. Gao, G. Wang, S. Miao, H. Wu, J. Li and X. Bao, *J. Mater. Chem. A*, 2014, **2**, 20067-20074.